

# Time-Domain Compression of Complex-Baseband LTE Signals for Cloud Radio Access Networks

Karl F. Nieman and Brian L. Evans

Wireless Networking and Communications Group, The University of Texas at Austin, Austin, TX

Email: karl.nieman@utexas.edu, bevans@ece.utexas.edu

**Abstract**—Modern cellular networks such as Long-Term Evolution (LTE) transport complex-baseband samples between remote radio hardware and processing equipment. Common Public Radio Interface (CPRI) links are widely used in practice and enable flexible radio head deployments, distributed antenna systems, and advanced spatial processing such as coordinated multi-point (CoMP) transmission and reception. Current CPRI links already have insufficient capacity to support 20 MHz bandwidth LTE for a basestation with three sectors and four antennas per sector. By supporting eight antennas per sector and up to  $5\times$  system bandwidth, LTE-A will require substantial increases in CPRI capacity. In this work, we develop compression methods that exploit the temporal and spectral structure of LTE signals with the goal of achieving high compression with limited impact on end-to-end communication performance. Our contributions include (i) design of a low-complexity compression method for LTE and (ii) validation of this method using an LTE link-level simulation. Our method achieves up to  $5\times$  compression for uplink and downlink signals.

## I. INTRODUCTION

Common public radio interface (CPRI) is a cooperative industrial standard for high-bandwidth serial data links [1]. CPRI links are used to transfer digital complex-baseband wireless signals to/from radio equipment and basestation processors and can be implemented over electrical or optical interfaces. CPRI links allow multiple radio equipment (antennas) and bands (carriers) to be aggregated and distributed amongst processing units. This allows the formation of distributed antenna systems and processing networks and can be used for cooperative multi-point (CoMP) transmission and reception [2]. Most ( $>90\%$ ) of available CPRI line bandwidth (see Table I) is used for complex-baseband data samples.

Traditional cellular networks are realized using stand-alone basestations and static coverage cells. A cloud radio access network (C-RAN) reinvents this concept in order to provide increased energy efficiency and collaboration [3]. C-RAN envisions large-scale shared radio and computational resources, affording more efficient hardware use on an as-needed basis and allowing for a cleaner, more energy-efficient network. As shown in Fig. 1, a collection of remote radio heads (RRHs) and basestation (BS) processing units share baseband sample data over CPRI links. This data can be routed to idle BSs to serve user equipment (UEs) in a virtual coverage area, affording flexibility in processing and the virtualization of network resources.

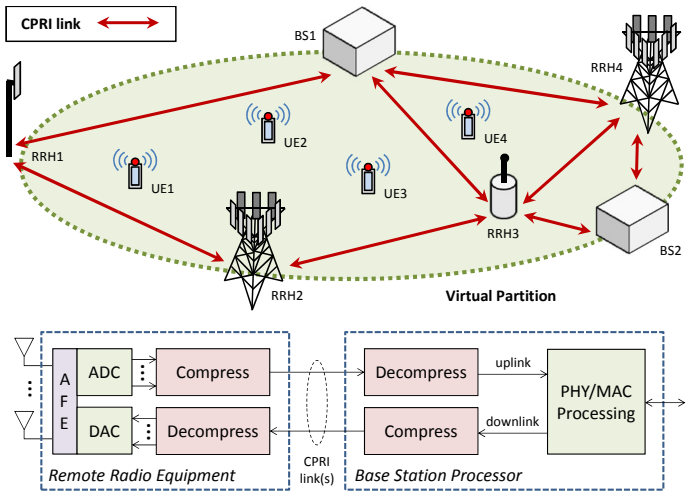


Fig. 1. (top) CPRI connects remote radio heads (RRHs) and basestation (BS) processors to serve a virtual (and potentially dynamic) coverage area. Coordinated Multi-Point (CoMP) processing serving user equipment (UEs) can be distributed amongst BSs using the CPRI network. (bottom) CPRI compression for baseband wireless signals.

The evolution of modern RANs with CoMP and future C-RAN architectures necessitates the availability of less expensive, higher bandwidth links to transfer complex-baseband samples. In this work, we develop compression methods that exploit the time and frequency structure of LTE signals to lower line rate requirements per site with minimal impact on overall communication performance.

## II. LTE SIGNAL STRUCTURE

LTE downlink signals are modulated using orthogonal frequency division multiple access (OFDMA) and uplink signals are modulated using single carrier frequency-division multiple access (SC-FDMA). In the OFDMA (downlink) case, subcarrier symbols are drawn from an  $M$ -QAM (quadrature amplitude modulation) symbol set where  $M \in \{4, 16, 64\}$ . For SC-FDMA, this symbol set is precoded using a length-12 discrete Fourier transform (DFT) and is scaled by the channel. If uplink power control is implemented, mean uplink transmit power remains the same across subcarriers.

TABLE I  
AVAILABLE CPRI LINE BIT RATES

CPRI option	1	2	...	6	7
Bit rate (Gbit/s)	0.614	1.229	...	6.144	9.830

This research is supported by Huawei.

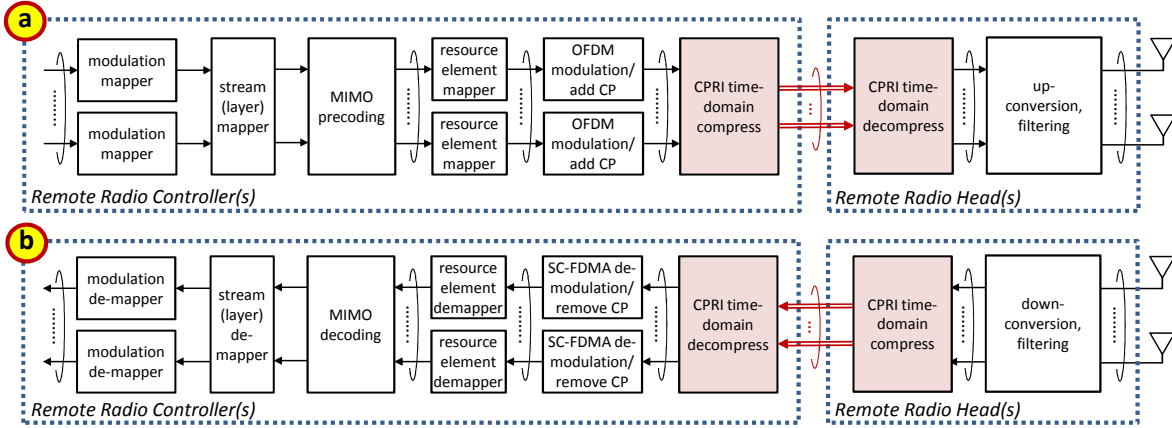


Fig. 2. Time-domain compression applied between the remote radio head and the remote radio controllers for (a) downlink and (b) uplink LTE signals.

Subcarriers are grouped into contiguous blocks of 12 and allocated to users over a subframe duration (1 ms) in an atomic unit known as a radio resource block. User allocation can exist across across spatial layers for multi-user MIMO transmission and can span the time-frequency grid according to scheduling allocations. LTE is designed to operate in different bandwidths as shown in Table II but shares similar time/frequency structure across operating modes. Each LTE mode has empty subcarriers in  $\sim 2/5$  of their spectrum at the upper and lower band edge known as guard subcarriers. These subcarriers are zeroed to lengthen the transition region and ease front-end anti-aliasing filter design. In typical LTE systems, CPRI samples are represented by 30 bits per sample with 15 bits per real and imaginary part.

Compression of LTE uplink and downlink signals can be achieved by exploiting redundancies in the signal structure. As shown in Fig. 2, uplink compression is applied after down conversion and downlink compression is applied after the bulk of the physical layer processing. Compression methods for LTE complex-baseband samples are surveyed in [3]. These techniques include methods such as sample rate reduction to the Nyquist rate and non-linear quantization. Frequency domain are discussed, though issues are cited with control signaling and increased complexity at the RRH.

Time-domain compression techniques for baseband signals is discussed in [4]. In this work, samples are converted to block floating point representation and rate converted. Dithering is used across parallel links to reduce compression error. An aggregate rate reduction of  $3\times$  is achieved. Simplify Systems, Inc., a commercial compression solutions vendor, advertises a compression rate of up to  $4\times$  using their proprietary Prism IQ product [5], details of which are not publicly available. Lloyd-Max quantizers, which take advantage of the statistical structure of the baseband signals, are discussed in [6], though few details are provided about their use in LTE. Lloyd-Max quantization minimizes mean squared error using a potentially non-uniform spacing depending on the probability density function (PDF) of the amplitude. In [7], distributed compression is achieved for baseband uplink signals using the conditional Karhunen-Loève Transform.

TABLE II  
SPECIFICATIONS FOR 5, 10, AND 20 MHz LTE SIGNALS

Channel bandwidth (MHz)	5	10	20
Frame duration (ms)	10		
Subframe duration (ms)	1		
Subcarrier spacing (kHz)	15		
Sampling frequency (MHz)	7.68	15.36	30.72
FFT size	512	1024	2048
Occupied subcarriers (incl. DC subcarrier)	301	601	1201
Guard subcarriers	211	423	847
Number of resource blocks	25	50	100
Occupied channel bandwidth (MHz)	4.515	9.015	18.015
OFDM symbols/subframe	7/6 (short/long CP)		
CP length (short CP) ( $\mu\text{s}$ )	5.2 (symbol 0)/ 4.69 (symbols 1-6)		
CP length (long CP) ( $\mu\text{s}$ )	16.67		

### III. SPECTRAL-TEMPORAL COMPRESSION

In OFDMA, a vector of  $X = \{X_k\}$ ,  $k = 0, 1, \dots, N - 1$  allocated subcarriers are encoded as  $M$ -QAM symbols. In SC-FDMA, these symbols are precoded using a DFT. Since there is sufficient whitening and scrambling of  $X$ , these symbols can be assumed to be *i.i.d.* samples drawn from a scaled  $M$ -QAM constellation. In a natural application of the Lindberg-Lévy Central Limit Theorem (CLT), for a sufficiently large IFFT length  $N$ , the resulting amplitude statistics of the real and imaginary component converge to a circular Gaussian amplitude distribution:

$$\left. \begin{aligned} & \sqrt{N} \text{Re} \left( \left[ \frac{1}{N} \sum_{k=0}^{N-1} X_k \omega_N^{kn} \right] - \mu \right) \\ & \sqrt{N} \text{Im} \left( \left[ \frac{1}{N} \sum_{k=0}^{N-1} X_k \omega_N^{kn} \right] - \mu \right) \end{aligned} \right\} \xrightarrow{d} \mathcal{N}(0, \sigma^2/2). \quad (1)$$

Here,  $\frac{1}{N} \sum_{k=0}^{N-1} X_k \omega_N^{kn}$  denotes the  $N$ -length inverse discrete Fourier transform of  $X$  where  $\omega_N = e^{j2\pi/N}$  is the  $N^{\text{th}}$  root of unity. A similar result can be shown for SC-FDMA with power control for large  $N$ .

For sufficient IFFT length, OFDMA samples can be modeled as a Gaussian process. However, in the LTE case, samples are not *i.i.d.*. Since LTE signals are oversampled—i.e. the process does not have uniform power spectral density over all frequencies—correlation exists in the time-domain. Despite this correlation, a scalar quantizer can be designed that is optimal in the minimum mean squared error (MMSE) sense for samples with a given amplitude PDF [8]. In this case, we consider an  $L$ -level quantizer designed for a Gaussian distribution with zero-mean and variance  $\sigma^2$ . Decision thresholds for this quantizer are expressed as

$$t_q = \frac{1}{2} (\hat{x}_{q-1} + \hat{x}_q), \quad q = 1, 2, \dots, L-1. \quad (2)$$

To ensure MMSE optimality, quantization levels are derived to be the centroid of each decision region—i.e.

$$\hat{x}_q = \frac{\int_{t_q}^{t_{q+1}} x f_X(x) dx}{\int_{t_q}^{t_{q+1}} f_X(x) dx}, \quad q = 0, 1, \dots, L-1. \quad (3)$$

In Cartesian representation, the threshold levels for the real and imaginary parts of samples drawn from a Gaussian PDF can be derived using the inverse  $Q$ -function. The quantization levels are derived to be

$$\hat{x}_q = \frac{N\sigma}{\sqrt{2\pi}} \left[ e^{-\frac{1}{2}t_j^2} - e^{-\frac{1}{2}t_{j+1}^2} \right], \quad q = 0, 1, \dots, L-1. \quad (4)$$

In polar coordinates, of the Gaussian optimized quantizer can be derived using separate magnitude and phase PDFs. The magnitude follows the Rayleigh distribution and the phase PDF is uniform over  $[-\pi, \pi]$ . The quantizer for the magnitude can be shown to be

$$t_q = \sqrt{-2\sigma^2 \ln \left( 1 - \frac{q}{L} \right)}, \quad q = 1, 2, \dots, L-1, \quad (5)$$

and the quantization levels are derived as shown in (7). Results from these derivations are used to set threshold levels and form look up tables for quantization and inverse quantization. These steps are denoted by  $Q$  and  $Q^{-1}$  in Fig. 2.

$$t_q = -Q^{-1} \left( \frac{\sigma q}{L} \right), \quad q = 1, 2, \dots, L-1, \text{ for even } L. \quad (6)$$

Though the Gaussian-optimized quantizer is optimal in the MMSE sense for the PDF of the amplitude of OFDMA signals, baseband LTE signals are still oversampled by a factor of  $\sim 1.5\times$ . This can be exploited to further improve signal-to-quantization noise ratio (SQNR) and allow for increased compression. To allow for noise shaping, a filter structure is introduced in an error-feedback loop. Introducing feedback of this filtered error signal modifies the noise transfer function of the system, allowing for quantization noise to be shaped. Noise shaping is widely used in audio signal processing to push noise into parts of the audible band that our ears are less

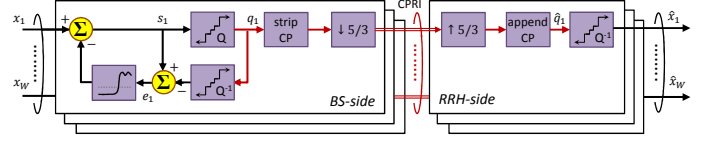


Fig. 3. Time-domain LTE downlink compression method optimized for amplitude statistics. Non-uniform quantization via Lloyd-Max quantization is performed in addition to noise-feedback coding. Rates are further reduced by puncturing samples and converting the rate to Nyquist. Compressed data is then sent across CPRI and reconstructed at the RRH using an inverse mapping and sample reconstruction. The process is reciprocal for uplink.

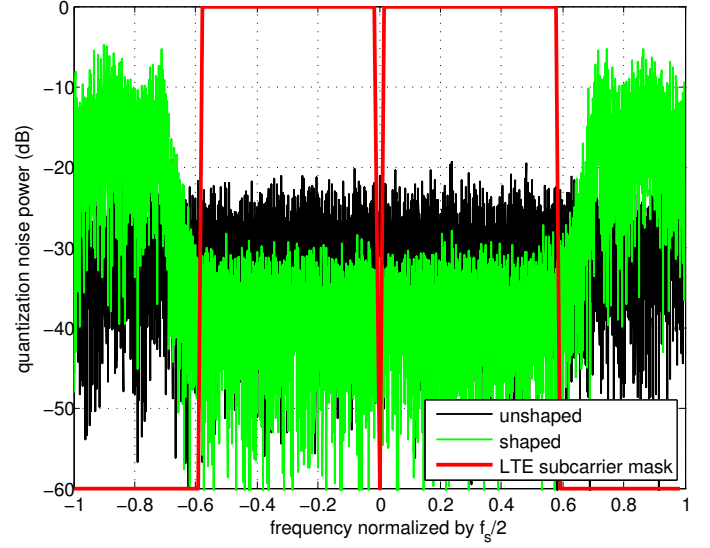


Fig. 4. A noise shaping filter used in a 5-bit Gaussian-optimized quantizer designed for LTE signals. Noise is reshaped to guard bands, improving in-band SQNR by an average of 6 dB across subcarriers.

sensitive to while preserving high SQNR in more sensitive parts of the spectrum [9]. Fig. 4 shows the effects of noise shaping for a  $L = 2^5$  (5-bit) Gaussian quantizer loop. The filter was designed for LTE signal structure to reshape noise power to LTE guard bands. The designed filter is a fifth-order Chebyshev Type II IIR filter. Using noise feedback with this filter results in an improved in-band SQNR of 6 dB and allows for a further reduction of wordlength by 1 bit. Block scaling can be performed before the quantizer stage and a gain factor can be added to a block of samples to ensure in range values for a fixed quantizer.

Samples output from this compression stage are still rate-matched to the input sample rate. Total rate can be further reduced by stripping off cyclic prefix (CP) samples in the downlink and decimating by a factor of  $\frac{5}{3}$  using a multi-rate filter. Throughput is reduced by an additional factor of  $\sim 1.78\times$  by removing these redundancies. Samples removed in this stage can be replaced using an inverse process on the other side of the CPRI link.

$$\hat{x}_q = \sqrt{2\pi\sigma^2 L} \left\{ \left[ \operatorname{erf} \left( \frac{t_{q+1}}{\sqrt{2\sigma^2}} \right) - \operatorname{erf} \left( \frac{t_q}{\sqrt{2\sigma^2}} \right) \right] - \left( t_{q+1} e^{\frac{t_{q+1}^2}{2\sigma^2}} - t_q e^{\frac{t_q^2}{2\sigma^2}} \right) \right\}, \quad q = 0, 1, \dots, L-1. \quad (7)$$

#### IV. SIMULATION RESULTS

A compression testbench was constructed using the LTE Link Level Simulators developed at the Vienna University of Technology [10]. The uplink simulator was modified to include compression/decompression blocks after the channel (at the BS input) and the downlink simulator was modified to include compression/decompression blocks within the BS before transmission to the UE. Two performance metrics are used in our evaluation of the compression methods discussed in Section III. First, coded bit error rates (BERs) are recorded to measure the impact on end-to-end link level performance. Second, error vector magnitude (EVM) is measured as specified in Annex E of [11] to be less than the LTE requirements 17.5%, 12.5%, and 8% for QPSK, 16-QAM, and 64-QAM, respectively. The most sensitive (highest SNR) channel quality index (CQI) of 15 (64-QAM, code rate = 938/1024) was used for both uplink and downlink simulations. Downlink was simulated over an additive white Gaussian noise (AWGN) channel using 5 MHz LTE, and uplink was simulated over the PedA channel using 1.4 MHz LTE. The simulator was run for 500 subframes for each configuration.

Fig. 5 shows the resulting BER curves for several compression methods on (a) downlink and (b) uplink signals. The word length specified is the number of bits used per complex-baseband sample as measured before the rate change after the quantizer structure in Fig. 3. As shown in the figure, our methods achieve a reduction from 30 to 10 bits wordlength per sample. The Gaussian w/ noise-shaping feedback method achieves an EVM of  $<2\%$ , exceeding the minimum EVM specification in [11] and achieving similar BER performance for a typical LTE SNR range. Both non-uniform quantization and noise shaping each afford the reduction of one bit in word length for similar BER performance. After quantization, further reduction in rate via cyclic prefix removal and rational rate change reduces the rate by an additional  $1.78\times$ , resulting in an overall reduction of  $5.3\times$ . Further compression is possible for lower CQIs due to higher code rate and modulation.

#### V. CONCLUSION

We have applied a combination of rescaling, non-uniform quantization, noise-shaping error feedback, and resampling to compress LTE uplink and downlink signals. Our low-complexity, time-domain methods achieve up to  $5\times$  compression versus standard 15-bit complex-baseband representation and can be readily implemented in digital logic. Future work will exploit spatial compressibility for multiple antennas.

#### REFERENCES

- [1] CPRI Specification V.5.0(2011-09-21), "Common Public Radio Interface (CPRI); Interface Specification," 2011.
- [2] J. Zhang, R. Chen, J. Andrews, A. Ghosh, and R. Heath, "Networked MIMO with clustered linear precoding," *IEEE Transactions on Wireless Communications*, vol. 8, no. 4, pp. 1910–1921, 2009.
- [3] China Mobile Research Institute, "C-RAN: The road towards green RAN," 2011.
- [4] D. Samardzija, J. Pastalan, M. MacDonald, S. Walker, and R. Valenzuela, "Compressed transport of baseband signals in radio access networks," *IEEE Transactions on Wireless Communications*, vol. 11, no. 9, pp. 3216–3225, 2012.

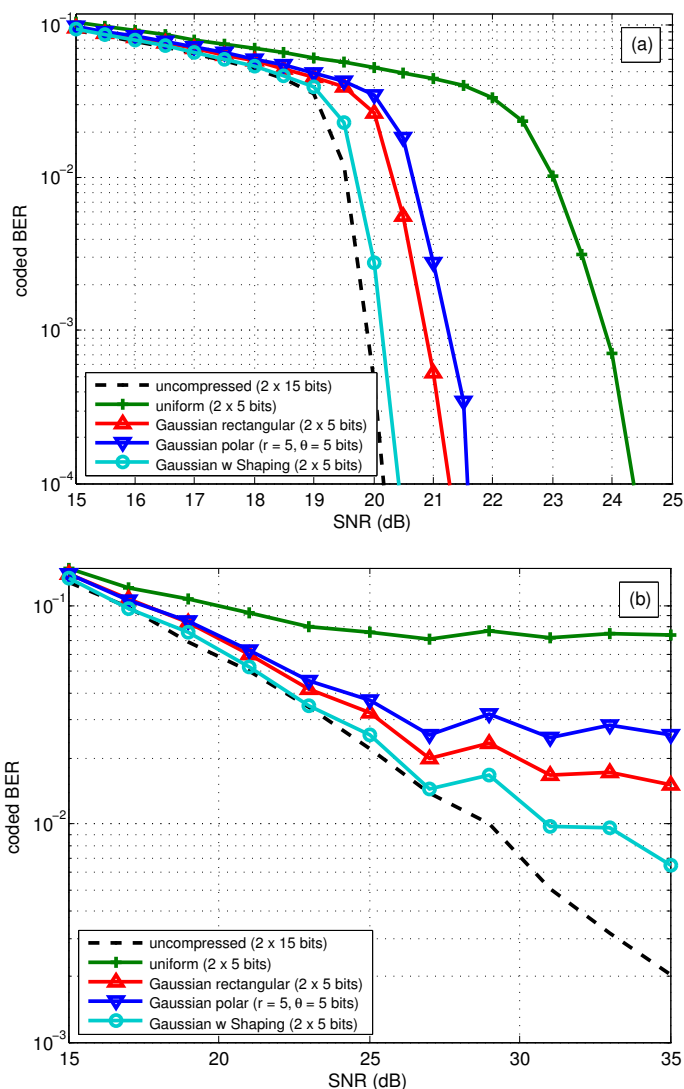


Fig. 5. Coded bit-error-rate (BER) for time-domain compression methods applied on LTE (a) downlink signals with CQI = 15, bandwidth = 5 MHz, AGWN channel and (b) uplink signals with CQI = 15, bandwidth = 1.4 MHz, PedA channel. BER is decreased using non-uniform quantization and noise-shaping. The *Gaussian w Shaping* method achieves performance close to that of the uncompressed signal.

- [5] A. W. Wegener, "Compression of baseband signals in base transceiver system interfaces," Patent US8 320 433 B2, 2011.
- [6] TD Industry Alliance, "Vision," pp. 37–40, March 2012, in Chinese. [Online]. Available: <http://www.tdia.cn/shijie/201203.pdf>
- [7] S.-H. Park, O. Simeone, O. Sahin, and S. Shamai, "Robust and efficient distributed compression for cloud radio access networks," *Vehicular Technology, IEEE Transactions on*, vol. 62, no. 2, pp. 692–703, 2013.
- [8] A. Gersho and R. M. Gray, *Vector Quantization and Signal Compression*. Springer, 1992.
- [9] D. De Koning and W. Verhelst, "On psychoacoustic noise shaping for audio requantization," in *Acoustics, Speech, and Signal Processing, 2003. Proceedings. (ICASSP '03). 2003 IEEE International Conference on*, vol. 5, 2003, pp. V–453–6 vol.5.
- [10] C. Mehlführer, J. C. Ikuno, M. Šimko, S. Schwarz, M. Wrulich, and M. Rupp, "The Vienna LTE simulators - enabling reproducibility in wireless communications research," *EURASIP Journal on Advances in Signal Processing*, vol. Vol. 2011, pp. 1–13, 2011.
- [11] "3GPP Technical Specification Group Radio Access Network; Evolved Universal Terrestrial Access Network (E-UTRA); Base Station Radio Transmission and Reception (Release 11)," 2013.